Article

Cells of Origin in the Embryonic Nerve Roots for NF1-Associated Plexiform Neurofibroma

Zhiguo Chen,[1] Chiachi Liu,[1] Amish J. Patel,[1,2] Chung-Ping Liao,[1] Yong Wang,[1] and Lu Q. Le[1,3,4,*]
[1]Department of Dermatology
[2]Cancer Biology Graduate Program
[3]Harold C. Simmons Cancer Center
[4]UTSW Neurofibromatosis Clinic
University of Texas Southwestern Medical Center, Dallas, TX 75390-9133, USA
*Correspondence: lu.le@utsouthwestern.edu
http://dx.doi.org/10.1016/j.ccell.2014.09.009

SUMMARY

Neurofibromatosis type 1 is a tumor-predisposing genetic disorder. Plexiform neurofibromas are common NF1 tumors carrying a risk of malignant transformation, which is typically fatal. Little is known about mechanisms mediating initiation and identity of specific cell type that gives rise to neurofibromas. Using cell-lineage tracing, we identify a population of GAP43^{+} PLP[+] precursors in embryonic nerve roots as the cells of origin for these tumors and report a non-germline neurofibroma model for preclinical drug screening to identify effective therapies. The identity of the tumor cell of origin and facility for isolation and expansion provides fertile ground for continued analysis to define factors critical for neurofibromagenesis. It also provides unique approaches to develop therapies to prevent neurofibroma formation in NF1 patients.

INTRODUCTION

The tumor predisposition disorder Neurofibromatosis type I (NF1) is among the most common human genetic diseases and is caused by mutation in the *NF1* tumor suppressor gene, which encodes a GTPase Activating Protein (GAP) that negatively regulates p21-RAS signaling (Ballester et al., 1990; Xu et al., 1990). NF1 patients have defects in neural crest-derived tissues, leading to a wide spectrum of clinical presentations, including developmental, pigment or neoplastic aberrations of the skin, nervous system, bones, endocrine organs, blood vessels, and the eyes (Cichowski and Jacks, 2001; Ward and Gutmann, 2005; Zhu et al., 2001). While NF1 patients are predisposed to developing multiple tumor types (Cichowski et al., 1999; Jett and Friedman, 2010; Le and Parada, 2007; Shannon et al., 1994; Vogel et al., 1999), the most common occurring are neurofibromas. Neurofibromas are unique and complex tumors that contain proliferating Schwann-like cells and other local supporting elements of the nerve fibers, including perineurial cells, fibroblasts, and blood

vessels, as well as infiltration of mast cells. Neurofibromas are classified into different subtypes. However, for clinical and prognostic implications, many clinicians simply refer to these tumors as either dermal or plexiform. Dermal neurofibromas are exclusively in the skin and occur in virtually all individuals with NF1. They initially appear at puberty and increase in number with age. Although similar to dermal neurofibromas at the cellular and ultrastructural levels, plexiform neurofibromas develop along a nerve plexus or involve multiple nerve bundles and are capable of forming large tumors. Unlike their dermal counterpart, plexiform neurofibromas are thought to be congenital and progressively enlarge throughout life. They carry a risk of malignant transformation that can metastasize widely and are often fatal. Plexiform neurofibromas can occur anywhere along peripheral nerve plexus. In fact, deep-tissue neurofibromas occur in 20%–40% of adult NF1 patients (Tonsgard et al., 1998). The majority of internal plexiform neurofibromas manifest in the para-spinal region associated with dorsal root ganglia (DRG). Their chance of malignant transformation is much higher compared with other

---

Significance

In this study, we utilized a genetically engineered mouse model as a tool to identify the cell of origin for plexiform neurofibroma. Using cell-lineage tracing, we showed that the embryonic GAP43^{+} PLP[+] Schwann cell precursors originate from spinal nerve roots are the cells of origin for plexiform neurofibromas. Our studies point to the importance of stem cells and their immediate progenitors in the initiation of tumors, consistent with the notion that these neoplasms originate in a subset of primitive precursors and that most cells in an organ do not generate tumors. Identifying which cell type gives rise to a particular cancer (the cells of origin) will permit greater understanding of their pathogenesis and inform better design approaches for their treatment.

forms of plexiform neurofibromas and carries a poorer prognosis, in part because they are not evident clinically in the early stage. In addition, because of their location at the neural foramina of the vertebral column, they can impinge on the spinal cord and nerve roots, causing pain and neurological deficits. Thus, these para-spinal neurofibromas represent a serious complication of NF1.

A large body of direct and indirect studies has provided evidence that *NF1* gene deletion is the requisite initial step that precedes the cascade of interactions with other cell types in the microenvironment as well as additional cell autonomous modifications for neurofibromagenesis (Joseph et al., 2008; Le et al., 2009; Wu et al., 2008; Zheng et al., 2008; Zhu et al., 2002). Early speculation regarding the cells of origin for neurofibromas came from genetic studies examining the participation of different cell types including neural crest derivatives in the pathogenesis of many of the clinical presentations of NF1, including neurofibroma. In human neurofibromas, Schwann-like cells with biallelic *NF1* mutations are the most consistently found cell type, leading to the argument that the tumors initiate in Schwann cells or their earlier precursors. Indeed, genetic mouse models have demonstrated that *Nf1* deletion in the Schwann cell lineage is the genetic bottleneck for neurofibroma development (Cichowski et al., 1999; Joseph et al., 2008; Vogel et al., 1999; Wu et al., 2008; Zheng et al., 2008; Zhu et al., 2002).

During the development of peripheral nerves, neural crest cells generate Schwann cells in a process that parallels embryonic development. Migrating neural crest stem cells emerge from the dorsal horns of the neural tube and move through immature connective tissue before the time of nerve formation and then differentiate into Schwann cell precursors (SCPs). These SCPs then become immature Schwann cells in the developing peripheral nerves until early neonatal stages. The differentiation of immature Schwann cells to form the non-myelinating and myelinating cells of mature nerves essentially occurs postnatally (Jessen and Mirsky, 2005; Woodhoo and Sommer, 2008). Given that the majority of plexiform neurofibromas in human are congenital and generally detected at birth or in early infancy, they must arise from the early Schwann cell lineage. Indeed, genetic mouse models have demonstrated that *Nf1* deletion in the embryonic Schwann cell lineage is the genetic bottleneck for neurofibroma development (Cichowski et al., 1999; Joseph et al., 2008; Vogel et al., 1999; Wu et al., 2008; Zheng et al., 2008; Zhu et al., 2002). However, the exact developmental stage and embryonic location of the Schwann cell lineage that initiate neurofibroma formation remain unknown. NF1 patients frequently have plexiform neurofibromas in the para-spinal region at the neural foramina associated with DRG. In addition, existing mouse models of NF1 also develop neurofibromas at the DRG regions. We wish to identify the cells of origin for these para-spinal plexiform neurofibromas. We reason that they reside in the vicinity of the embryonic DRGs or at the nearby nerve roots.

RESULTS

Loss of *Nf1* in Embryonic DRG/Nerve Root Neurosphere Cells Gives Rise to Classic Plexiform Neurofibroma In Vivo

Recent studies have established the value of in vitro sphere assay to identify cancer stem cells as well as neural stem/progenitor cells (Le et al., 2009; Williams et al., 2008). Therefore, we examined whether *Nf1*-deficient embryonic DRG/nerve root neurosphere cells (DNSCs) could contain the elusive cells of origin of para-spinal neurofibromas. To obtain *Nf1*$^{-/-}$ DNSCs, we dissected DRGs/nerve roots from E13.5 *Nf1*$^{flox/flox}$; *Rosa26(R26R)* mouse embryos (Hall, 2006) and performed the neurosphere culture. These neurosphere cells have high self-renewal and proliferative potential (Figures S1A–S1D available online). They were subsequently infected with adenovirus carrying the *Cre* recombinase (*Ad-CMV-Cre*) to ablate *Nf1* and generate *Nf1*$^{-/-}$;*LacZ*$^+$ DNSCs, which was verified by genomic analysis of *Nf1* (Figure 1A).

We next implanted *Nf1*$^{-/-}$;*LacZ*$^+$ DNSCs into the sciatic nerves where close proximity to the nerve environment could be achieved as previously established through an in vivo neurofibromagenesis assay (Le et al., 2009). The transplanted *Nf1*$^{-/-}$;*LacZ*$^+$ DNSCs gave rise to plexiform neurofibroma within four months post implantation, whereas the transplanted *Nf1*$^{flox/flox}$;*R26R* controls showed no signs of tumor growth (Figures 1Ba–1Bd and Table 1). These tumors exhibited all histological and immunohistochemical features of human plexiform neurofibromas, including disorganized spindle cells, abundant collagen matrix, heavy infiltration of mast cells and macrophages, expression of the Schwann cell marker S100β, and GAP43 (Figure 1C; Figure S1E). To verify these tumors arise from transplanted DRG/nerve root neurosphere cells rather than from the host cells, we took advantage of the fact that the transplant cells carried the *LacZ* marker gene but the host did not. X-gal staining shown that these tumor cells were LacZ$^+$, which suggested that they arose from transplanted *Nf1*$^{-/-}$;*LacZ*$^+$ DNSCs. Taken together, these data indicate that when placed in a favorable microenvironment (in proximity to a peripheral nerve), *Nf1*$^{-/-}$;*LacZ*$^+$ DNSCs can give rise to bona fide plexiform neurofibromas. As such, these results show that DNSCs have the full potential to generate neurofibromas and indicate that the cells of origin for para-spinal neurofibromas may be in the embryonic DRGs/nerve roots.

Cells of Origin for Para-Spinal Plexiform Neurofibromas Are inside the Embryonic PLP$^+$ Cells

Although we successfully induced neurofibroma formation by transplanting embryonic *Nf1*$^{-/-}$ DNSCs to sciatic nerves, it is unlikely that all the embryonic DNSCs could give rise to plexiform neurofibroma. In genetic mouse models, *Nf1* ablation in embryonic Schwann cell lineage (PLP, Krox20, and DHH positive cells) was sufficient to induce para-spinal plexiform neurofibromas (Le et al., 2011; Wu et al., 2008; Zhu et al., 2002), suggesting that all or at least part of the cells of origin might be inside these PLP$^+$, Krox20$^+$, and DHH$^+$ embryonic Schwann cell lineage. Therefore, we next sought to determine this subpopulation within the embryonic DNSCs that could give rise to neurofibroma.

To achieve this, we crossed *Plp* promoter-driven, tamoxifen-inducible Cre (*PlpCre-ERT*) (Leone et al., 2003) transgenic mice into a *Nf1*$^{flox/flox}$;*R26R-LacZ* (Le et al., 2011) and *Flox-stop-Flox R26R-YFP* (Chen et al., 2009) background to generate *PlpCre-ERT;Nf1*$^{flox/flox}$;*R26R-LacZ-YFP* mice. We selectively ablated the embryonic *Nf1* expression by administering 1 mg tamoxifen orally at embryonic day 11.5 (E11.5) to pregnant *Nf1*$^{flox/flox}$;*R26R-LacZ-YFP* female mice that have been bred

A

B

C

Table 1. The Cells of Origin for Spinal Plexiform Neurofibroma Are inside the Embryonic PLP⁺ DNSCs

Genotype	DNSCs	Selected Ablation of *Nf1*	Tumors/Nude Mice Injected	Percentage	p Value
Nf1^f/f^;*LacZ*	total	*Ad-Cre*	5/6	83.3	0.015
	total	*Ad-GFP*	0/6	0	
PlpCre-ERT; Nf1^f/f^;*LacZ-YFP*	YFP⁺		13/20	65	<0.001
	YFP⁻		2/20	10	
PlpCre-ERT; Nf1^f/f^;*LacZ-YFP*	YFP⁺	*Ad-Cre*	13/18	72.2	<0.001
	YFP⁻	*Ad-Cre*	3/21	14.3	
Krox20-Cre; Nf1^f/f^;*LacZ-YFP*	YFP⁺		13/15	86.7	<0.001
	YFP⁻		3/15	20	
Krox20-Cre; Nf1^f/f^;*LacZ-YFP*	YFP⁺	*Ad-Cre*	11/14	78.6	0.678
	YFP⁻	*Ad-Cre*	9/14	64.3	
Dhh-Cre; Nf1^f/f^;*LacZ-YFP*	Total	*Ad-Cre*	11/16	68.8	1
	YFP⁻	*Ad-Cre*	12/16	75	

Figure 1. Loss of *Nf1* in Embryonic DNSCs Gives Rise to Classic Plexiform Neurofibroma In Vivo

(A) Diagram of experimental design: Isolation of DRGs/nerve roots from E13.5 *Nf1*^flox/flox^;*R26R-LacZ* embryos (a) and DNSCs culture (b); DNSCs were infected with *Ad-Cre* to ablate *Nf1*; *Ad-GFP* was used as a control (c); and *Nf1*^−/−^;LacZ⁺ and *Nf1*^flox/flox^;LacZ⁻ DNSCs were implanted to right and left sciatic nerves of nude mice, respectively (d).

(B) X-gal and H&E staining were performed on left (a and b) and right (c and d) sciatic nerve.

(C) Tumor on right sciatic nerve was stained with antibody against S100β and GAP43.

Blue scale bars, 500 μm. White and black scale bars, 50 μm. See also Figure S1.
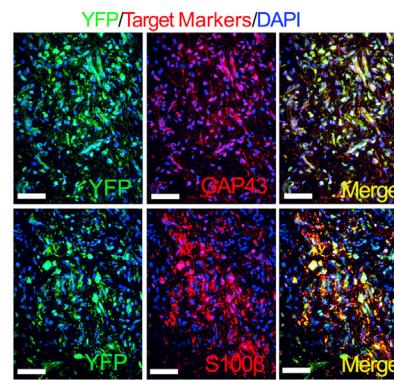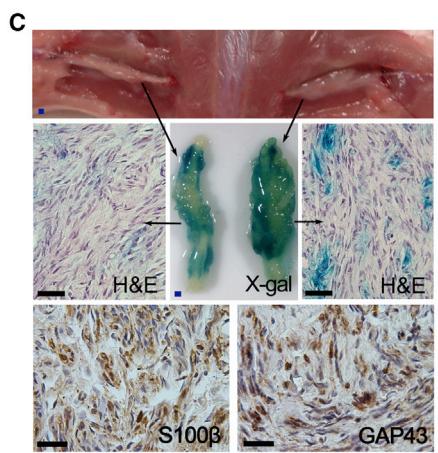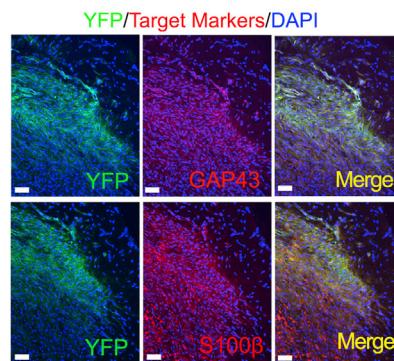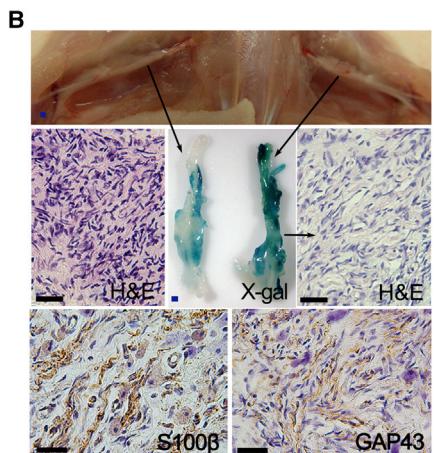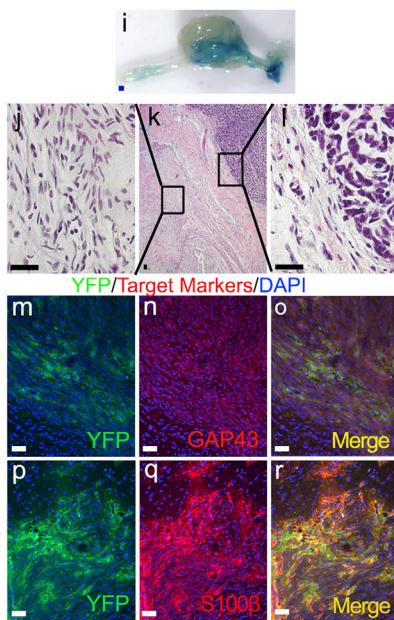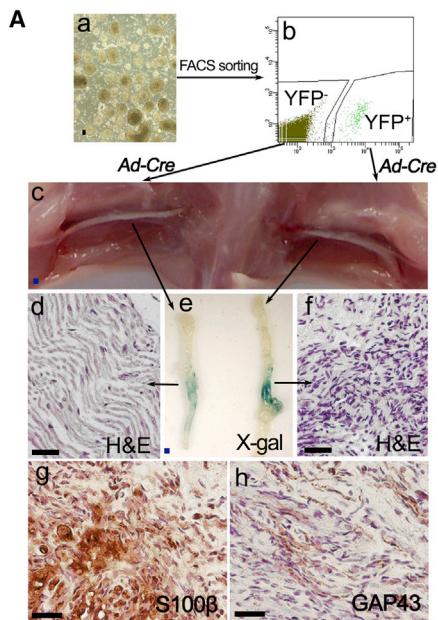
with *PlpCre-ERT;Nf1*^flox/flox^;*R26R-LacZ-YFP* male mice. We then dissected the DRGs/nerve roots from embryos at E13.5 and performed DNSCs culture. In order to isolate the PLP⁺ and PLP⁻ from these E13.5 DNSCs, we used fluorescence-activated cell sorting (FACS) to obtain the YFP⁺ and YFP⁻ DNSCs which represented PLP⁺ and PLP⁻ DNSCs, respectively. Next, these PLP⁺ and PLP⁻ DNSCs were transplanted in proximity to the sciatic nerve of nude mice. Thirteen of 20 (65%) mice transplanted with PLP⁺ DNSCs developed sciatic plexiform neurofibroma (Table 1). By contrast, PLP⁻ DNSCs only led to neurofibroma in 2 of 20 (10%) mice (Table 1), which suggests that PLP⁺ DNSCs are more likely than PLP⁻ DNSCs to contain the cells of origin and that neurofibroma development in the PLP⁻ DNSCs implanted mice is likely the result of contamination of PLP⁺ DNSCs during the sorting process as loss of *Nf1* is required for neurofibroma development. Therefore, given that the *Nf1* have been ablated in PLP⁺ DNSCs and not in PLP⁻ DNSCs after the tamoxifen induction, we could not exclude the possibility that *Nf1* ablation in PLP⁻ DNSCs would also give rise to neurofibroma. To address this issue, both PLP⁺ and PLP⁻ DNSCs were infected with *Ad-CMV-Cre* to generate the PLP⁺;*Nf1*^−/−^ and PLP⁻;*Nf1*^−/−^ DNSCs. When transplanted to the sciatic nerve of nude mice, PLP⁺; *Nf1*^−/−^ DNSCs maintained their higher capability to give rise to neurofibroma (13 of 18, 72.2%), whereas PLP⁻;*Nf1*^−/−^ DNSCs could only give rise to plexiform neurofibroma in 3 out of 21 (14.3%) mice (Figure 2A and Table 1). Strikingly, we also observed spontaneous transformation into malignant peripheral nerve sheath tumors (MPNST) arising from a fraction of these sciatic plexiform neurofibromas that originated from PLP⁺; *Nf1*^−/−^ DNSCs (Figures 2Ai–2Al). This is consistent with human clinical observations that about 10% of plexiform neurofibromas undergo malignant transformation (Evans et al., 2002). These data further indicate that the cells of origin might be within the embryonic PLP⁺ DNSCs population.

However, since *Nf1* ablation in Krox20⁺ and DHH⁺ embryonic Schwann cell lineage could also give rise to para-spinal plexiform neurofibromas, we next examined whether the cells of origin are also inside the embryonic Krox20⁺ or DHH⁺ DNSCs (Wu et al., 2008; Zhu et al., 2002). We utilized the same strategies as above using the *Krox20-Cre* and *Dhh-Cre* transgenic mice. Unexpectedly, we found that not only the Krox20⁺;*Nf1*^−/−^ and total DNSCs (contained DHH⁺;*Nf1*^−/−^ DNSCs) but also the

Figure 2. The Cells of Origin for Para-Spinal Plexiform Neurofibroma Are inside the Embryonic PLP⁺ DNSCs

(A) FACS was performed to obtain the YFP⁺ and YFP⁻ DNSCs from E13.5 *PlpCre-ERT;Nf1*^flox/flox^*; R26R-LacZ-YFP* embryo, whose mother was administered with tamoxifen at E11.5 (a and b). Both YFP⁺ and YFP⁻ DNSCs were infected with *Ad-Cre* to ablate *Nf1*, then injected to right and left sciatic nerves of nude mice respectively (c). X-gal and H&E staining were performed on the left and right sciatic nerve (d–f). Sections of right sciatic nerve were stained with antibody against S100β (g) and GAP43 (h). A fraction of these sciatic plexiform neurofibromas spontaneously transformed into MPNST, exhibiting both benign and malignant histologic characters (i–l). Immunofluorescence staining of tumor on right sciatic nerve shows expression of YFP as well as GAP43 and S100β Schwann cell markers (m–r).

(B and C) A similar strategy to that in (A) was used for YFP⁺ and YFP⁻ DNSCs derived from E13.5 embryos with genotype *Krox20-Cre;Nf1*^flox/flox^*; R26R-LacZ-YFP* (B) and *Dhh-Cre;Nf1*^flox/flox^*; R26R-LacZ-YFP* (C).

Blue scale bars, 500 μm. White and black scale bars, 50 μm.

DNSCs might only account for partial population of the cells of origin.

The PLP⁺ Cells of Origin Originate in the Embryonic Nerve Roots

To determine if the embryonic Krox20⁺ and DHH⁺ cells are included within PLP⁺ cell population, we administered tamoxifen orally to mother mice at E11.5 to activate *PlpCre-ERT* to induce the expression of YFP and genetically label the PLP⁺ cells. We next performed immunofluorescence staining against Krox20 and DHH and observed that the majority of the endogenous Krox20 and DHH signals colocalized with YFP (PLP) in the nerve root, DRG, and peripheral nerve (Figure 3A), which indicated that most of the Krox20⁺ and DHH⁺ cells were included in the PLP⁺ cell population. We also found that PlpCre⁺ (YFP⁺ cells) colocalized with endogenous PLP, suggesting that the PlpCre⁺ population is inside the endogenous PLP⁺ cell population (Figure S2A).

We then took advantage of another marker, LacZ, to compare the specific expression pattern of LacZ among *Plp*, *Krox20*, and *Dhh* Cre mice. Specifically, for embryos with genotype *PlpCre-ERT;R26R-LacZ*, we gave the mother mice a single dose of 4-hydroxytamoxifen, an active metabolic product of tamoxifen that can be cleared relatively quickly from serum

Krox20⁻*;Nf1*⁻/⁻ and DHH⁻*;Nf1*⁻/⁻ DNSCs gave rise to neurofibroma with high percentage (Figures 2B and 2C and Table 1). These results demonstrate that PLP⁺ DNSCs encompass the cells of origin pool, whereas Krox20⁺*;Nf1*⁻/⁻ and DHH⁺*;Nf1*⁻/⁻
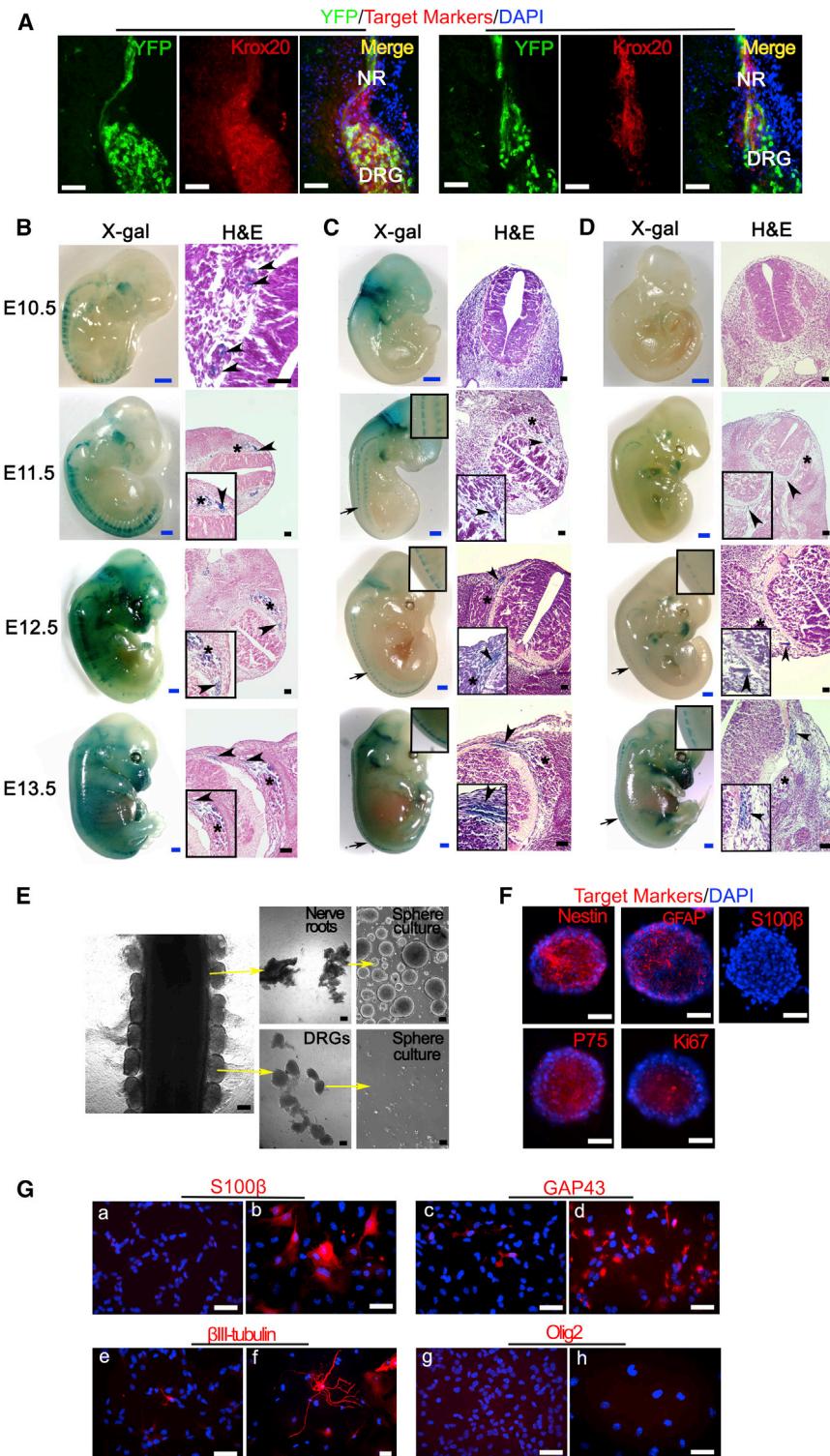
Figure 3. Cells of Origin for Para-Spinal Plexiform Neurofibromas Are inside the Embryonic PLP⁺ Nerve Root Cells

(A) Representative frozen sections from E13.5 *PlpCre-ERT;Nf1*flox/flox*;R26R-LacZ-YFP* embryo, whose mother was administered with tamoxifen at E11.5, were stained for YFP, Krox20, DHH, and DAPI. NR, nerve root; DRG, dorsal root ganglia.

(B–D) X-gal and H&E staining were performed on embryos with genotype *PlpCre-ERT;R26R-LacZ* (B, mother mouse was administered with 4-hydroxytamoxifen at E9.5), *Krox20-Cre;R26R-LacZ* (C), and *Dhh-Cre;R26R-LacZ* (D) from E10.5 to E13.5. Arrow, area of enlarged view; arrow head, nerve roots; star mark, DRG.

(E) DRG and dorsal nerve root were separated from E13.5 embryos and cultured in neurosphere culture conditions.

(F) Nerve root derived neurospheres immunostained for Nestin, GFAP, S100β, P75, Ki67, and DAPI.

(G) Immunostaining of nerve root derived neurosphere cells cultured in neurosphere medium (a, c, e, and g) or differentiation medium (b, d, f, and h) with antibodies against S100β, GAP43, βIII-tubulin, and Olig2.

Blue scale bars, 500 μm. White and black scale bars, 50 μm. See also Figure S2.

to show up inside the nerve roots, DRGs, and trigeminal ganglion (TG) at E10.5 (Figure 3B). Histological analysis indicated that the LacZ⁺ (PLP⁺) cells were mainly inside the nerve roots and only few scattered LacZ⁺ (PLP⁺) cells could be seen in DRG (Figure 3B). From E11.5 to E13.5, more LacZ⁺ (PLP⁺) cells appear in nerve roots, DRGs, TGs, and eventually peripheral nerves (Figure 3B). In contrast, in the *Krox20-Cre* mice, the LacZ⁺ (Krox20⁺) cells first appear in nerve roots at E11.5 and stay in nerve roots until E13.5 when some peripheral nerves started to express the LacZ (Krox20). However, there were very few LacZ⁺ (Krox20⁺) cells inside the DRG (Figure 3C). Similarly, in *Dhh-Cre* mice, we could only observe very few LacZ⁺ (DHH⁺) cells in nerve roots after E11.5. From E12.5 to E13.5, more LacZ⁺ (DHH⁺) cells were detected only at nerve roots and some of the peripheral nerves (Figure 3D), which were consistent with previous findings that *Dhh* transcripts were expressed by SCPs both in the dorsal and ventral roots at E13 (Parmantier et al., 1999). All of these data suggest that the PLP⁺ cells first appear in embryonic nerve roots at least one day earlier and in a wider cell population than that of Krox20⁺ and DHH⁺ cells and that PLP⁺ DNSCs represent a wider pool for the cells of origin. Consistently, when we carefully separated out the E13.5

(Robinson et al., 1991), to acutely induce the expression of LacZ in PLP⁺ cells at E9.5. On the other hand, *Krox20-Cre* and *Dhh-Cre* are noninducible and, therefore, tamoxifen induction is not needed. We isolated the embryos at different time points and performed whole-mount X-gal staining. For the *PlpCre-ERT;R26R-LacZ* mice, the LacZ (PLP) positive staining began
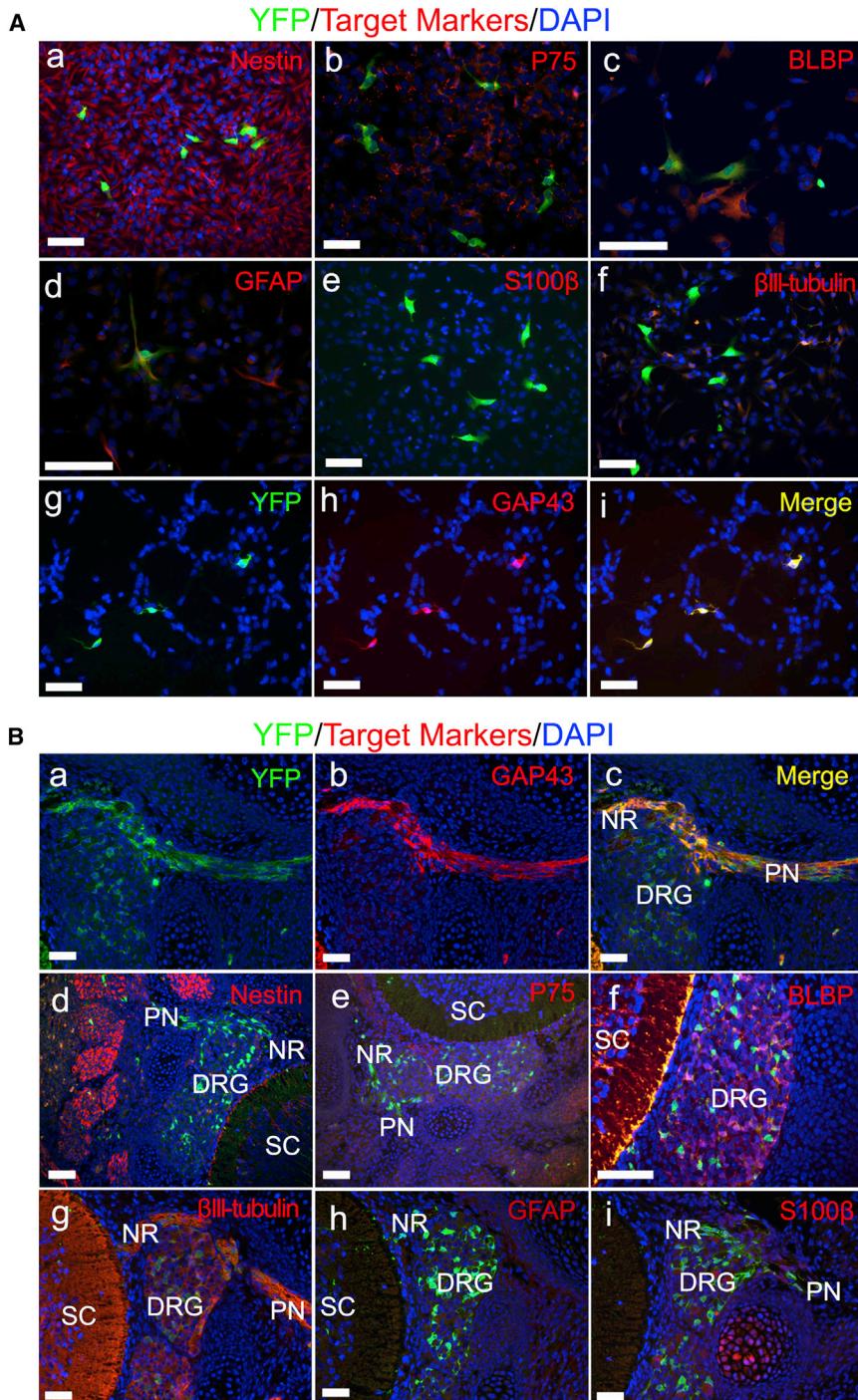
Figure 4. Phenotypic Analysis Identifies the PLP+ Cells of Origin as Embryonic Schwann Cell Precursors

(A) DNSCs obtained from E13.5 *PlpCre-ERT; Nf1*flox/flox*;R26R-YFP* embryos, whose mother was administered with tamoxifen at E11.5, were stained for YFP, DAPI, and lineage markers: Nestin (a), P75 (b), BLBP (c), GFAP(d), S100β (e), βIII-tubulin (f), and GAP43 (g–i).

(B) Formalin fixed paraffin embedded sections from E13.5 *PlpCre-ERT;Nf1*flox/flox*;R26R-YFP* embryos, whose mother was administered with tamoxifen at E11.5, were stained for YFP, DAPI, and lineage markers: GAP43 (a–c), Nestin (d), P75 (e), BLBP (f), βIII-tubulin (g), GFAP (h), and S100β (i). DRG, dorsal root ganglia; NR, nerve root; PN, peripheral nerve; SC, spinal cord.

All scale bars, 50 μm. See also Figure S3.

Under differentiation conditions, these neurosphere cells could differentiate into Schwann cells and neurons, but not the oligodendrocytes (Figure 3G). These data further narrow the candidate cells of origin to PLP+ cells in the embryonic nerve roots.

Phenotypic Analysis Identifies the PLP+ Cells of Origin as Embryonic Schwann Cell Precursors

Boundary cap (BC) cells are transient neural crest-derived population of stem cells located at the dorsal root entry zone and give rise to most Schwann cells in the dorsal roots and DRGs (Coulpier et al., 2009; Hjerling-Leffler et al., 2005; Topilko et al., 1994). Therefore, BC cells might be the embryonic neurofibroma tumor cells of origin. However since Krox20 is a marker of BC cells and both Krox20+; $Nf1^{-/-}$ and Krox20−;$Nf1^{-/-}$ DNSCs could give rise to sciatic plexiform neurofibroma, this indicates that BC cells are unlikely to be the cells of origin, but rather an even earlier cell that is PLP+. To phenotypically characterize these PLP+ cells of origin, we gavaged mother mice with tamoxifen at E11.5, harvested DRGs/nerve roots from *PlpCre-ERT;Nf1*flox/flox*; R26R-YFP* embryos at E13.5 for neuro-

embryonic dorsal nerve roots from the DRGs, we found that only the embryonic dorsal nerve roots could robustly give rise to neurospheres, but not the E13.5 DRGs (Figure 3E). However, in adult mice, we found that the DRGs can also give rise to neurospheres (Figure S2B). Further immunofluorescence analyses demonstrate that these embryonic nerve roots generated neurosphere cells that express neural crest markers (Nestin and P75), immature Schwann cell marker GFAP, and proliferation marker Ki-67, but not the mature Schwann cell marker S100β (Figure 3F).

sphere cell culture, and performed immunofluorescence analyses. We found that the majority of neurosphere cells, either YFP+(PLP+) or YFP−(PLP−), expressed Nestin and P75, which confirms that they originate from the neural crest (Figures 4Aa and 4Ab). We also observed the expression of embryonic Schwann cell markers BLBP and GFAP in the minority of both YFP+(PLP+) and YFP−(PLP−) cells, but none expressed the immature and mature Schwann cell marker S100β (Figures 4Ac–A4e). In addition, the majority of YFP+(PLP+) cells did not

Figure 5. Cell Lineage Tracing Reveals PLP+ Precursors in the Embryonic Nerve Roots as the Cells of Origin for Plexiform Neurofibromas

(A) X-gal staining of whole spinal cord, DRGs and partial peripheral nerves from *PlpCre-ERT; Nf1*^flox/−^*;R26R-LacZ* mouse, whose mother was administered with tamoxifen at E9.5. There is strong X-gal staining in the enlarged DRGs (star mark), enlarged intercostal nerve (arrow head), and nerve root (arrow).

(B) H&E and immunohistochemical staining for GAP43 and S100β in sections from these enlarged LacZ+ DRGs (star mark in A).

(C) H&E staining of the DRG and its associated enlarged intercostal nerve (EIN) in (A) (arrow head). Enlarged intercostal nerve was also stained for GAP43 and S100β.

(D) Representative H&E and immunohistochemical analyses of early neurofibroma in dorsal root and associated normal DRG (arrow in A). DRG, dorsal root ganglia; DR, dorsal root; SC, spinal cord; VR, ventral root.

Blue scale bars, 500 μm. All other scale bars, 50 μm.

express neuronal marker βIII-tubulin (Figure 4Af). Strikingly, every YFP+(PLP+) cell also expressed GAP43, a Schwann cell marker that is known to first appear at the precursor stage (Figures 4Ag–4Ai), and Sox10, a marker for neural crest origin and future Schwann cell lineage (Figure S3A) (Kalcheim and Rohrer, 2014). Because these PLP+GAP43+ cells are also P75 positive but S100β negative, they are at Schwann cell precursor stage (Jessen and Mirsky, 2005). It is well known that cell culture in vitro may vary from that in vivo. Therefore, we also characterized these PLP+ cells in E13.5 *PlpCre-ERT;Nf1*^flox/flox^*;R26R-YFP* embryos and observed that YFP+(PLP+) cells were colocalized with GAP43 mainly at nerve roots (Figures 4Ba–4Bc). Similar to our in vitro data, they also expressed Nestin, P75, BLBP, and Sox10 (Figures 4Bd–4Bf; Figure S3B). They were also colocalized with βIII-tubulin (Figure 4Bg). However, they did not express GFAP and S100β in vivo (Figures 4Bh and 4Bi). These findings indicate that PLP+GAP43+ cells in the embryonic nerve roots are SCPs and that they may be the elusive cells of origin for para-spinal plexiform neurofibroma.

Cell Lineage Tracing Confirms the PLP+ Precursors Originate in the Embryonic Nerve Roots as the Cells of Origin for Plexiform Neurofibromas

Tumor cells of origin are difficult to identify by characterizing cells within terminal stage tumors. A more definitive approach is to genetically label specific lineage early in development for fate tracing prior to tumorigenesis. X-gal staining demonstrates that LacZ+(PLP+) cells are mainly located in nerve roots at E10.5 when we gave 4-hydroxytamoxifen to pregnant mother mice at E9.5 (Figure 3B). If these *Nf1* ablated LacZ+(PLP+) nerve root cells would give rise to neurofibroma, then neurofibroma cells should carry the marker gene *LacZ*. Therefore, we crossed *PlpCre-ERT;Nf1*^flox/flox^*;R26R-LacZ* male mice with *Nf1*^flox/−^*;R26R-LacZ* female mice. We then administered 4-hydroxytamoxifen to pregnant mother mice for one dose at E9.5. At 7 months of age, *PlpCre-ERT;Nf1*^flox/−^*;R26R-LacZ* progenies from these crosses began to show classic signs of illness: lethargy, weight loss, and paralyzed hind limbs. We observed the presence of plexiform neurofibromas with strong positive X-gal staining in close proximity to the cervical and thoracic DRGs (Figure 5A). Because *PlpCre-ERT* mediates labeling solely at the time of tamoxifen administration at E9.5, X-gal positive staining of neurofibroma cells demonstrates unambiguously that the labeled neurofibromas were derived from E9.5 PLP+ precursors in the embryonic nerve roots. Histopathological analysis of these tumors indicated that the tumors exhibited cardinal features of plexiform neurofibromas (Figure 5B). Strikingly, we also observed plexiform neurofibroma developed along the intercostal nerve whose associated DRG appears histologically normal (Figure 5C). In addition, we identified the earliest form of neurofibroma exhibiting LacZ positive staining: classic pathological characteristics of neurofibroma and expressing Schwann cell marker S100β and GAP43 at the dorsal nerve roots near the DRG (Figure 5D). Together, these findings point to the PLP+;GAP43+ SCPs in the embryonic nerve roots as the cells of origin for plexiform neurofibroma.
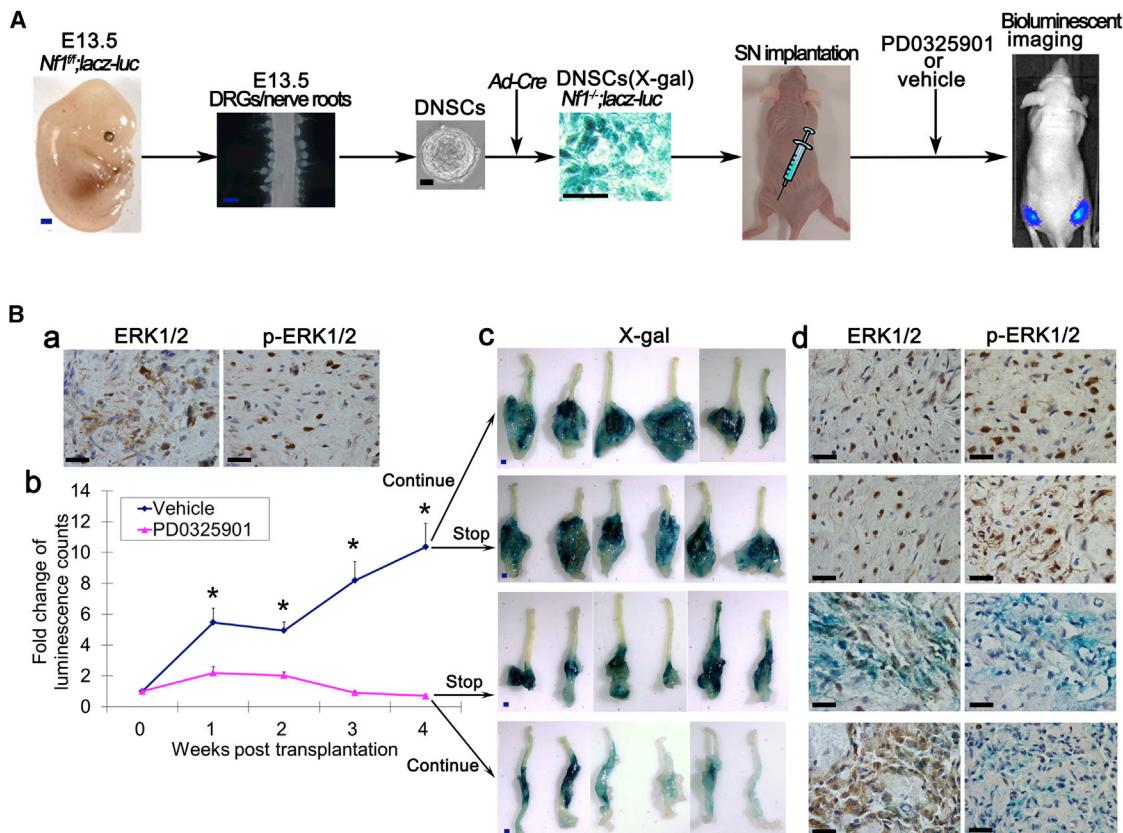
Figure 6. Therapeutic Effect of MAPK Signaling Inhibitor on DNSC-Derived Plexiform Neurofibroma

(A) Diagram of experimental design for testing therapeutic effect of PD0325901 on plexiform neurofibroma.

(B) Immunostaining of ERK1/2 (total) and p-ERK1/2 (phosphorylated ERK) in E13.5 $Nf1^{-/-}$ DNSCs derived sciatic plexiform neurofibroma (a). Fold change of luminescence count measured during PD0325901 or vehicle treatment (b). After 4 weeks of treatment, both PD0325901 and vehicle treatment group were divided into two subgroups: discontinued PD0325901 or continued PD0325901 and discontinued vehicle treatment or continued vehicle treatment subgroups for an additional 4 weeks. Tumors were then harvested for X-gal staining (c) and immunostaining for ERK1/2 and p-ERK1/2 (d). Statistics were represented as the mean ± SEM (*p < 0.05).

Blue scale bars, 500 μm. All other scale bars, 50 μm. See also Figure S4.

A Robust Plexiform Neurofibroma Model for Preclinical Drug Screening

The *Nf1* gene encodes for neurofibromin, a Ras GTPase activating protein (GAP), and thus negatively regulates the RAS signaling pathway (Rubin and Gutmann, 2005). This has prompted the use of specific MAP Kinase pathway inhibitors to counteract *Nf1* loss-mediated tumor development (Chang et al., 2013; Jessen et al., 2013; Staser et al., 2013) or to treat *Nf1* mutant animals in the effort to restore abnormal brain development and cognitive function (Li et al., 2012; Lush et al., 2008; Wang et al., 2012). To determine if our non-germline plexiform neurofibroma model could be used as a rapid preclinical therapeutic drug screening tool to identify effective therapies, we used a highly selective pharmacological inhibitor of MEK, PD0325901, which blocks activation and phosphorylation of ERK1/2 (Chang et al., 2013), to test whether inhibition of the Ras/Raf/MEK/ERK signaling pathway can prevent neurofibroma progression in our plexiform neurofibroma model.

In order to monitor the proliferation of tumor cells, we labeled these neurofibroma cells with Luciferase by crossing the *Nf1*^flox/flox*;R26R-LacZ* (Le et al., 2011) mice with *Flox-stop-Flox*

R26R-Luciferase mice to generate *Nf1*^flox/flox*;R26R-LacZ-Luciferase* mice. We then harvested E13.5 DNSCs and infected with *Ad-CMV-Cre* to generate *Nf1*^−/−*;R26R-LacZ-Luciferase* DNSCs. We transplanted these *Nf1*^−/−*;R26R-LacZ-Luciferase* DNSCs to sciatic nerves of nude mice to generate plexiform neurofibromas. Mice were randomly assigned to PD0325901 treatment (5 mg/kg/day, 5 day/week) or vehicle as a control group (Figure 6A). We also tested if the MAPK pathway is activated in our neurofibromas and found that the ERK pathway is highly activated in the tumor tissues as shown by immunohistochemistry analysis (Figure 6Ba). We then started the treatment right after the transplantation. A striking reduction in luciferase signal was observed even after only one week of PD0325901 treatment (p < 0.01). Continued treatment of PD0325901 further inhibited the proliferation of tumor cells. After 4 weeks of PD0325901 treatment, tumor cell proliferation was almost completely blunted as demonstrated by the diminishing luciferase signal. On the other hand, the luciferase signal in vehicle treatment group increased more than 10 times after 4 weeks of treatment (Figure 6Bb). These data suggested that the PD0325901 could effectively inhibit the proliferation of plexiform neurofibroma.

However, it was not clear whether the inhibition effect of PD0325901 would be sustained after stopping the PD0325901 treatment. To answer this question, we divided the PD0325901 treatment group into two subgroups: discontinued PD0325901 treatment after 4 weeks or continued PD0325901 treatment for an additional 4 weeks in another group of mice. Similar to this, we also divided the vehicle treatment group into two subgroups based on continuing or discontinuing vehicle treatment for another 4 weeks. We again used the luciferase signal as a surrogate marker for tumor growth. We observed that continued treatment of PD0325901 further blunted the proliferation of neurofibroma; however, they regained the proliferative capacity after PD0325901 withdrawal. Eight weeks after transplantation of DNSCs, we sacrificed all mice and performed X-gal staining of the sciatic nerves. Vehicle treatment groups (8 weeks or 4 weeks) developed very large LacZ$^+$ neurofibromas, 4-week PD0325901 treatment dramatically reduced the growth of neurofibromas, while 8-week PD0325901 treatment almost completely prevented the proliferation of neurofibroma (Figure 6Bc; Figure S4). Consistently, ERK1/2 phosphorylation was also reduced in both PD0325901 treatment groups compared with vehicle treatment groups (Figure 6Bd). All of these data showed the requirement of sustained Ras/Raf/MEK/ERK signaling for neurofibroma growth and that continuous PD0325901 treatment is effective in restraining this growth. Thus, our non-germline plexiform neurofibroma model provides a powerful approach for preclinical therapeutic drug screening to identify effective therapies for human clinical trials to prevent neurofibroma formation in NF1 patients, where none exist today.

DISCUSSION

Recent progress in cancer research points to the importance of stem cells and their immediate progenitors in the initiation and maintenance of many tumors, consistent with the notion that these neoplasms originate in a subset of primitive precursor cells and that most cells in an organ do not generate tumors (Alcantara Llaguno et al., 2009; Barker et al., 2009; Bonnet and Dick, 1997; Chen et al., 2012a; Goldstein et al., 2010; Le et al., 2009; Reya et al., 2001; Tysnes, 2010). Identifying which cell type gives rise to a particular cancer (the cells of origin) will permit greater understanding of their pathogenesis and inform better design approaches for their treating. In this study, we utilized a genetically engineered mouse model as a tool to identify the cells of origin for plexiform neurofibroma. Using cell lineage tracing, we demonstrated that the embryonic PLP$^+$;Nf1$^{-/-}$ SCPs, which originate from spinal nerve roots, give rise to plexiform neurofibroma not only in para-spinal areas but also in distal peripheral nerve. We also report a non-germline model for plexiform neurofibroma that can be used broadly as preclinical models for therapeutic testing.

A large body of direct and indirect studies has provided evidence that Nf1 gene deletion is the requisite initial step that precedes neurofibromagenesis (Joseph et al., 2008; Le et al., 2009; Wu et al., 2008; Zheng et al., 2008; Zhu et al., 2002). Cichowski et al. (1999) addressed this issue elegantly when they generated chimeric mice by injecting LacZ$^+$ Nf1$^{-/-}$ ES cells into wild-type blastocysts. These mice developed microscopic neurofibromas derived from the injected ES cells, demonstrating the requirement

of Nf1 homozygosity for tumor formation (Cichowski et al., 1999). However, the extent of chimerism in these mice occurs randomly and cannot be controlled genetically. As a result, it is difficult to establish the cells of origin for these tumors. Conditional deletion of Nf1 from embryonic neural crest stem cells (NCSCs) using Wnt-1-Cre transgenic mice leads to a transient increase in NCSC frequency and self-renewal, but the isolated NCSCs fail to form tumors upon transplantation (Joseph et al., 2008), suggesting that early NCSC derivatives may not contain potential cells of origin for plexiform neurofibroma. This observation indicates that later NCSC derivatives give rise to plexiform neurofibromas. Consistently, ablation of Nf1 in Schwann cells using P0A-Cre; Nf1$^{flox/-}$ or Dhh-Cre;Nf1$^{flox/flox}$ mice, which deletes Nf1 continuously from early SCPs through mature cells, efficiently induce neurofibromas development (Wu et al., 2008; Zheng et al., 2008). However, the Cre recombinase transgenes used in these two studies compromise Nf1 function at the early Schwann cell stages of development (at E12.5), and the Cre recombinase activity persists through the mature Schwann cell stage. Therefore, it is not possible to identify or exclude any particular Schwann cell developmental stage as the critical one for Nf1 loss-mediated tumor development. The interpretation of the data instead rests on correlations relating to detectable appearance of abnormal cells or structures. An alternative approach that can in theory provide a more precise evaluation of the evolution of NF1-associated tumors is the application of inducible Cre/loxP technology that allows temporal and spatial ablation of NF1 function in Schwann cells. Two different studies show that acute loss of Nf1 in both embryo and adult can lead to plexiform neurofibroma formation (Le et al., 2011; Mayes et al., 2011). The fact that Nf1 inactivation in adult mice also gives rise to neurofibroma, albeit at a much lower frequency (Le et al., 2011), indicates that either (1) mature Schwann cells can, in rare cases, give rise to neurofibroma or (2) that rare populations of progenitor cells persist within the adult peripheral nervous system.

The notion that mature Schwann cells have the capability to give rise to plexiform neurofibromas is less evident. NF1 patients rarely present with plexiform tumors for the first time as adults (Ferner, 2007). As aforementioned, Schwann cell development and terminal differentiation into myelinating cells mostly occurs postnatally. If mature Schwann cells as a whole can give rise to neurofibromas when loss of heterozygosity (LOH) occurs in adulthood, then it would be anticipated that plexiform tumors should develop widely in PlpCre-ERT mice induced postnatally since Cre-mediated recombination remains efficient in mature Schwann cells. It is not likely that the Schwann cell lineage undergoes immature to mature transition en masse at tightly defined times from the NCSC stage, to the precursor stage, to the immature stage, and onward to more differentiated stages. Instead, gradients of cells transition and migrate over extended periods with considerable overlap between the disappearance of one population and the emergence of another. Therefore, remaining compartments of precursor Schwann cells may also persist into adulthood and retain the capacity to form plexiform neurofibromas within the peripheral nerves. Indeed, given that embryonic nerve roots associate tightly with DRGs and that the harvested DRGs almost always contaminate with nerve roots, we carefully separated out the early embryonic dorsal nerve roots from the DRGs for neurosphere culture.

Unexpectedly, we found that only the embryonic dorsal nerve roots could robustly give rise to neurosphere but not the E13.5 DRGs. However, in adult mice, we found that the DRGs can give rise to neurospheres and neurofibroma when $Nf1$ was ablated and implanted into the sciatic nerves (data not shown). Consistently, when we acutely labeled the PLP$^+$ precursor cells with LacZ only in nerve roots at E10.5, we also observed plexiform neurofibroma developed in the peripheral nerve distal to the DRG. All of the data suggest that at least some of the cells of origin might migrate out along the nerve roots-DRG-peripheral nerve and retain the capacity to form neurofibroma later in life.

In the conditional knockout model using Cre/loxP technology, the $Krox20$-$Cre;Nf1^{flox/flox}$ mice (containing $Nf1^{-/-}$ Schwann cells and $Nf1^{+/+}$ microenvironment) do not develop neurofibromas. On the other hand, the $Krox20$-$Cre;Nf1^{flox/-}$ mice (containing $Nf1^{-/-}$ Schwann cells and $Nf1^{+/-}$ microenvironment) develop plexiform neurofibromas (Zhu et al., 2002), demonstrating the essential role for the heterozygous environment in the development of neurofibroma. In another mouse model, a more robust Dhh-Cre driver causes plexiform neurofibroma formation in an $Nf1$-wild-type background (Wu et al., 2008). In the current study, the PLP^+; $Nf1^{-/-}$ DNSCs could also effectively give rise to plexiform neurofibromas when transplanted into the sciatic nerves of nude mice, which also have an $Nf1$-wild-type background. It is important to emphasize here that under these conditions, a large group of SCPs undergoes $Nf1$ LOH simultaneously and can therefore vie with the wild-type environment more efficiently than when only one or a very few isolated SCPs undergo LOH. In NF1 patients that harbor germline heterozygous $NF1$ mutations, given the defined time of gestation and size of neural crest compartment, inactivation of the other normal $NF1$ in the Schwann cell lineage must be rare and stochastic, such that single cells undergo completely inactivation of $NF1$ in a large pool of otherwise heterozygous $NF1$ mutant cells. In this setting, the increased secretion of SCF or other factors from heterozygous cells, including mast cells, in the tumor microenvironment provides a permissive condition to foster tumor growth (Yang et al., 2008). Therefore, in the experimental setting, one possible advantage of having a large pool of precursors undergoing LOH would be a rapid and dramatic increase in cytokine and growth factor secretion that could be sufficient to elicit wild-type mast cells without the need for the hypersensitive heterozygous state of the latter. As such, in the physiologic scenario, one would envision a rare Schwann cell undergoing LOH that would normally disappear except for the response of the $Nf1$-heterozygous microenvironment that assists it to form a tumor. In another scenario, contribution of a multitude of cells that have undergone LOH may override the otherwise requisite contributions from other factors, such as heterozygous mast cells or other cells in the microenvironment, to induce neurofibroma development.

Although the tumor microenvironment is critical for neurofibroma formation (Le et al., 2009; Yang et al., 2008), intrinsic proliferative signals such as those in the MAPK pathways are equally essential. Therefore, both the tumor microenvironment and MAPK pathways have been targeted in the preclinical setting to define clinically relevant pharmacodynamic variables and evaluating duration of drug effects on individual tumor (Jessen et al., 2013; Yang et al., 2008). The purpose of preclinical drug screening is to select the most effective and safe compound

from a large library. Our non-germline model for plexiform neurofibroma enables high efficiency of tumorigenesis and has a much shorter latency. Therefore, it is a reliable and robust model for in vivo drug screening with a quantifiable and reproducible outcome measure (via bioluminescent scan) to select lead compounds for clinical assessment. In addition, the ability to isolate embryonic PLP$^+$ GAP43$^+$ cells for ex vivo expansion and $Nf1$ ablation to generate classic sciatic plexiform neurofibromas allows flexible and speedy manipulation with multiple genetic tools to delineate additional pathways that are perturbed upon the loss of $Nf1$, which are essential for neurofibroma development.

In conclusion, the identity of the tumor cells of origin and the facility for isolation and expansion for genetic alterations provide fertile ground for continued analysis to identify additional intrinsic and extrinsic factors within the tumor microenvironment that likely play essential roles in neurofibroma genesis. It is reasonable to speculate that lessons learned from investigating the molecular interactions between the neurofibroma cells of origin and their microenvironment will provide us approaches to develop effective therapies to delay and possibly prevent neurofibroma formation in NF1 patients.

EXPERIMENTAL PROCEDURES

Mice

Animal care and use were approved by the Institutional Animal Care and Use Committee at University of Texas Southwestern Medical Center. The $Nf1^{flox/-}$ and $Nf1^{flox/flox}$ mice have been described previously (Zhu et al., 2002). For conditional ablation of $Nf1$, we used a tamoxifen-inducible Cre line, the $PlpCre$-$ERT2$ transgenic mice (Leone et al., 2003), and two non-inducible Cre lines, $Krox20$-Cre and Dhh-Cre (Limpert et al., 2013; Zhu et al., 2002). The $Rosa26$-YFP reporter mice were described previously (Chen et al., 2009). The $ROSA26$-$lacZ$ and $ROSA26$-$Luciferase$ reporter mice were obtained from the Jackson Laboratories.

Tamoxifen and 4-Hydroxytamoxifen Induction

Tamoxifen (Sigma-Aldrich) and 4-hydroxytamoxifen was dissolved in a sunflower oil/ethanol mixture (9:1) at 10 mg/ml and 1 mg/ml, respectively. For embryonic induction, the pregnant mice were gavaged orally with 1 mg of tamoxifen or 0.2 mg of 4-hydroxytamoxifen at E11.5 or E9.5, respectively.

Cell Culture and Differentiation Assays

Mouse embryos were removed from anesthetized 13.5-day-old pregnant female mice. Embryos were sacrificed. The spinal cord of each embryo was removed, and DRGs/nerve roots were dissected from the vertebral column with the aid of stereomicroscope. Fine scissors was used to cut and separate the nerve roots and DRGs. DRG and/or nerve root neurosphere culture was performed as previously described (Le et al., 2009; Patel et al., 2014; Ratner et al., 2006). For cell proliferation assay, the single sphere cells were seeded to a 6-well plate coated with poly-D-lysine/laminin (4.0×10^3 cells per well) for monolayer culture. The cell numbers of 3 wells were counted every 24 hr for 5 days. For differentiation assays, we seeded 5.0×10^3 cells per well of an 8-chamber slide coated with poly-D-lysine/laminin and cultured with fresh media containing B27 + 5% fetal bovine serum for 7–14 days. Then we fixed the cells with 4% paraformaldehyde for 30 min and performed immunostaining for lineage markers.

Fluorescence-Activated Cell Sorting

We harvested YFP$^+$ and YFP$^-$ DNSCs using FACSAria instrument (BD Biosciences) equipped with a 488 nm solid-state laser.

Histology, Immunostaining, and X-Gal Staining

For hematoxylin and eosin (H&E) histology analysis, tissue specimens were harvested and fixed with 10% formalin in PBS for 1 day and subsequently

embedded in paraffin. Sections (5 μm thick) were stained with H&E per manufacturer's protocol (StatLab). The dilutions of primary antibodies used in immunohistochemistry and immunofluorescence studies were as follows: β III-tubulin (rabbit, 1:2000, Sigma-Aldrich), BLBP (rabbit,1:800, Millipore), CD31 (rabbit, 1:200, Abcam), BrdU (rat, 1:400, Abcam), Cleaved Caspase-3 (rabbit, 1:100, Cell Signaling Technology), DHH (rabbit,1:200, Santa Cruz Biotechnology), total ERK1/2 (rabbit,1:250, Cell Signaling Technology), phospho-ERK1/2 (rabbit,1:400, Cell Signaling Technology), GAP43 (rabbit, 1:1000, Abcam), GFAP (rabbit, 1:2000, DAKO), GFP (goat, 1:300, Rockland), Krox20 (rabbit, 1:200, Covance Research Products), Nestin (rabbit, 1:5000, Abcam), P75 (rabbit, 1:400, Millipore), PLP (rabbit, 1:800, Abcam), S100 β (rabbit, 1:5000, DAKO), Sox10 (Goat,1:400, Santa Cruz Biotechnology), and Vimentin (mouse, 1:800, Santa Cruz Biotechnology).

For X-gal staining, after total body perfusion with 4% paraformaldehyde, tissues or embryos were harvested, equilibrated in 30% sucrose in PBS overnight at 4°C, and stained with X-gal at 30°C overnight. The tissues were then postfixed with 10% formalin, paraffin embedded, sectioned, and counterstained with hematoxylin.

Transplantation Experiments

Sciatic nerve implantation of DNSCs was performed as previously reported (Chen et al., 2012b). Briefly, mice were anesthetized by intraperitoneal injection of 120 μl of a mixture of ketamine (10 mg/ml) and xylazine (1 mg/ml) solution. A skin incision was made above the femur. Using iris scissors, a pocket was created within the quadriceps muscles to expose the sciatic nerve. The 40 μl of L15 medium containing 1 × 10^6 viable DNSCs was then deposited into this pocket so that DNSCs can be in contact with the SN. The quadriceps muscles were then closed with 4-0 Vicryl suture, and the skin was closed with 5-0 prolene suture. Mice were allowed to recover from anesthesia, then subject to MEK Inhibitor treatment and bioluminescent imaging.

MEK Inhibitor Treatment

MEK inhibitor PD0325901 were kindly provided by Dr. Kevin Shannon. PD0325901 was dissolved in vehicle (0.5% hydroxypropyl methylcellulose with 0.2% Tween 80; Sigma-Aldrich) at a concentration of 1 mg/ml. The solution was administered orally at the dosage of 5 mg/kg (body weight) per mouse, once per day, for 5 days/week.

Bioluminescent Imaging

Bioluminescent imaging was performed as described previously (Chau et al., 2014). Briefly, mice were injected with 160 ul 20 mg/ml D-Luciferin Potassium Salt (Perkin Elmer) in 0.9% sterile NaCl, and total flux was quantified using IVIS Lumina II (Caliper Life Sciences) weekly.

Statistics

All data are displayed as the mean ± SEM unless specified otherwise. A two-tailed t test and Fisher exact test were applied as appropriate to evaluate statistical significance ($p < 0.05$ was deemed statistically significant).

SUPPLEMENTAL INFORMATION

Supplemental Information includes Supplemental Experimental Procedures and four figures and can be found with this article online at http://dx.doi.org/10.1016/j.ccell.2014.09.009.

AUTHOR CONTRIBUTIONS

L.Q.L. contributed to conception and experimental designs, data collection and/or assembly, data analysis and interpretation, manuscript writing, and final approval of manuscript. Z.C. contributed to experimental designs, data collection and/or assembly, data analysis and interpretation, and manuscript writing. C.L., A.J.P., C.-P.L., and Y.W. contributed to data collection.

ACKNOWLEDGMENTS

REFERENCES

Alcantara Llaguno, S., Chen, J., Kwon, C.H., Jackson, E.L., Li, Y., Burns, D.K., Alvarez-Buylla, A., and Parada, L.F. (2009). Malignant astrocytomas originate from neural stem/progenitor cells in a somatic tumor suppressor mouse model. Cancer Cell *15*, 45–56.

Ballester, R., Marchuk, D., Boguski, M., Saulino, A., Letcher, R., Wigler, M., and Collins, F. (1990). The NF1 locus encodes a protein functionally related to mammalian GAP and yeast IRA proteins. Cell *63*, 851–859.

Barker, N., Ridgway, R.A., van Es, J.H., van de Wetering, M., Begthel, H., van den Born, M., Danenberg, E., Clarke, A.R., Sansom, O.J., and Clevers, H. (2009). Crypt stem cells as the cells-of-origin of intestinal cancer. Nature *457*, 608–611.

Bonnet, D., and Dick, J.E. (1997). Human acute myeloid leukemia is organized as a hierarchy that originates from a primitive hematopoietic cell. Nat. Med. *3*, 730–737.

Chang, T., Krisman, K., Theobald, E.H., Xu, J., Akutagawa, J., Lauchle, J.O., Kogan, S., Braun, B.S., and Shannon, K. (2013). Sustained MEK inhibition abrogates myeloproliferative disease in Nf1 mutant mice. J. Clin. Invest. *123*, 335–339.

Chau, V., Lim, S.K., Mo, W., Liu, C., Patel, A.J., McKay, R.M., Wei, S., Posner, B.A., De Brabander, J.K., Williams, N.S., et al. (2014). Preclinical therapeutic efficacy of a novel pharmacologic inducer of apoptosis in malignant peripheral nerve sheath tumors. Cancer Res. *74*, 586–597.

Chen, J., Kwon, C.H., Lin, L., Li, Y., and Parada, L.F. (2009). Inducible site-specific recombination in neural stem/progenitor cells. Genesis *47*, 122–131.

Chen, J., Li, Y., Yu, T.S., McKay, R.M., Burns, D.K., Kernie, S.G., and Parada, L.F. (2012a). A restricted cell population propagates glioblastoma growth after chemotherapy. Nature *488*, 522–526.

Chen, Z., Pradhan, S., Liu, C., and Le, L.Q. (2012b). Skin-derived precursors as a source of progenitors for cutaneous nerve regeneration. Stem Cells *30*, 2261–2270.

Cichowski, K., and Jacks, T. (2001). NF1 tumor suppressor gene function: narrowing the GAP. Cell *104*, 593–604.

Cichowski, K., Shih, T.S., Schmitt, E., Santiago, S., Reilly, K., McLaughlin, M.E., Bronson, R.T., and Jacks, T. (1999). Mouse models of tumor development in neurofibromatosis type 1. Science *286*, 2172–2176.

Coulpier, F., Le Crom, S., Maro, G.S., Manent, J., Giovannini, M., Maciorowski, Z., Fischer, A., Gessler, M., Charnay, P., and Topilko, P. (2009). Novel features of boundary cap cells revealed by the analysis of newly identified molecular markers. Glia *57*, 1450–1457.

Evans, D.G., Baser, M.E., McGaughran, J., Sharif, S., Howard, E., and Moran, A. (2002). Malignant peripheral nerve sheath tumours in neurofibromatosis 1. J. Med. Genet. *39*, 311–314.

Ferner, R.E. (2007). Neurofibromatosis 1. Eur. J. Hum. Genet. *15*, 131–138.

Goldstein, A.S., Huang, J., Guo, C., Garraway, I.P., and Witte, O.N. (2010). Identification of a cell of origin for human prostate cancer. Science *329*, 568–571.

Hall, A.K. (2006). Rodent sensory neuron culture and analysis. Curr. Protoc. Neurosci. *Chapter 3*, Unit 3.19.

Hjerling-Leffler, J., Marmigère, F., Heglind, M., Cederberg, A., Koltzenburg, M., Enerbäck, S., and Ernfors, P. (2005). The boundary cap: a source of neural

crest stem cells that generate multiple sensory neuron subtypes. Development *132*, 2623–2632.

Jessen, K.R., and Mirsky, R. (2005). The origin and development of glial cells in peripheral nerves. Nat. Rev. Neurosci. *6*, 671–682.

Jessen, W.J., Miller, S.J., Jousma, E., Wu, J., Rizvi, T.A., Brundage, M.E., Eaves, D., Widemann, B., Kim, M.O., Dombi, E., et al. (2013). MEK inhibition exhibits efficacy in human and mouse neurofibromatosis tumors. J. Clin. Invest. *123*, 340–347.

Jett, K., and Friedman, J.M. (2010). Clinical and genetic aspects of neurofibromatosis 1. Genet. Med. *12*, 1–11.

Joseph, N.M., Mosher, J.T., Buchstaller, J., Snider, P., McKeever, P.E., Lim, M., Conway, S.J., Parada, L.F., Zhu, Y., and Morrison, S.J. (2008). The loss of Nf1 transiently promotes self-renewal but not tumorigenesis by neural crest stem cells. Cancer Cell *13*, 129–140.

Kalcheim, C., and Rohrer, H. (2014). Neuroscience. Following the same nerve track toward different cell fates. Science *345*, 32–33.

Le, L.Q., and Parada, L.F. (2007). Tumor microenvironment and neurofibromatosis type I: connecting the GAPs. Oncogene *26*, 4609–4616.

Le, L.Q., Shipman, T., Burns, D.K., and Parada, L.F. (2009). Cell of origin and microenvironment contribution for NF1-associated dermal neurofibromas. Cell Stem Cell *4*, 453–463.

Le, L.Q., Liu, C., Shipman, T., Chen, Z., Suter, U., and Parada, L.F. (2011). Susceptible stages in Schwann cells for NF1-associated plexiform neurofibroma development. Cancer Res. *71*, 4686–4695.

Leone, D.P., Genoud, S., Atanasoski, S., Grausenburger, R., Berger, P., Metzger, D., Macklin, W.B., Chambon, P., and Suter, U. (2003). Tamoxifen-inducible glia-specific Cre mice for somatic mutagenesis in oligodendrocytes and Schwann cells. Mol. Cell. Neurosci. *22*, 430–440.

Li, Y., Li, Y., McKay, R.M., Riethmacher, D., and Parada, L.F. (2012). Neurofibromin modulates adult hippocampal neurogenesis and behavioral effects of antidepressants. J. Neurosci. *32*, 3529–3539.

Limpert, A.S., Bai, S., Narayan, M., Wu, J., Yoon, S.O., Carter, B.D., and Lu, Q.R. (2013). NF-kappaB forms a complex with the chromatin remodeler BRG1 to regulate Schwann cell differentiation. J. Neurosci. *33*, 2388–2397.

Lush, M.E., Li, Y., Kwon, C.H., Chen, J., and Parada, L.F. (2008). Neurofibromin is required for barrel formation in the mouse somatosensory cortex. J. Neurosci. *28*, 1580–1587.

Mayes, D.A., Rizvi, T.A., Cancelas, J.A., Kolasinski, N.T., Ciraolo, G.M., Stemmer-Rachamimov, A.O., and Ratner, N. (2011). Perinatal or adult Nf1 inactivation using tamoxifen-inducible PlpCre each cause neurofibroma formation. Cancer Res. *71*, 4675–4685.

Parmantier, E., Lynn, B., Lawson, D., Turmaine, M., Namini, S.S., Chakrabarti, L., McMahon, A.P., Jessen, K.R., and Mirsky, R. (1999). Schwann cell-derived Desert hedgehog controls the development of peripheral nerve sheaths. Neuron *23*, 713–724.

Patel, A.J., Liao, C.P., Chen, Z., Liu, C., Wang, Y., and Le, L.Q. (2014). BET bromodomain inhibition triggers apoptosis of NF1-associated malignant peripheral nerve sheath tumors through Bim induction. Cell Reports *6*, 81–92.

Ratner, N., Williams, J.P., Kordich, J.J., and Kim, H.A. (2006). Schwann cell preparation from single mouse embryos: analyses of neurofibromin function in Schwann cells. Methods Enzymol. *407*, 22–33.

Reya, T., Morrison, S.J., Clarke, M.F., and Weissman, I.L. (2001). Stem cells, cancer, and cancer stem cells. Nature *414*, 105–111.

Robinson, S.P., Langan-Fahey, S.M., Johnson, D.A., and Jordan, V.C. (1991). Metabolites, pharmacodynamics, and pharmacokinetics of tamoxifen in rats and mice compared to the breast cancer patient. Drug Metab. Dispos. *19*, 36–43.

Rubin, J.B., and Gutmann, D.H. (2005). Neurofibromatosis type 1—a model for nervous system tumour formation? Nat. Rev. Cancer *5*, 557–564.

Shannon, K.M., O'Connell, P., Martin, G.A., Paderanga, D., Olson, K., Dinndorf, P., and McCormick, F. (1994). Loss of the normal NF1 allele from the bone marrow of children with type 1 neurofibromatosis and malignant myeloid disorders. N. Engl. J. Med. *330*, 597–601.

Staser, K., Park, S.J., Rhodes, S.D., Zeng, Y., He, Y.Z., Shew, M.A., Gehlhausen, J.R., Cerabona, D., Menon, K., Chen, S., et al. (2013). Normal hematopoiesis and neurofibromin-deficient myeloproliferative disease require Erk. J. Clin. Invest. *123*, 329–334.

Tonsgard, J.H., Kwak, S.M., Short, M.P., and Dachman, A.H. (1998). CT imaging in adults with neurofibromatosis-1: frequent asymptomatic plexiform lesions. Neurology *50*, 1755–1760.

Topilko, P., Schneider-Maunoury, S., Levi, G., Baron-Van Evercooren, A., Chennoufi, A.B., Seitanidou, T., Babinet, C., and Charnay, P. (1994). Krox-20 controls myelination in the peripheral nervous system. Nature *371*, 796–799.

Tysnes, B.B. (2010). Tumor-initiating and -propagating cells: cells that we would like to identify and control. Neoplasia *12*, 506–515.

Vogel, K.S., Klesse, L.J., Velasco-Miguel, S., Meyers, K., Rushing, E.J., and Parada, L.F. (1999). Mouse tumor model for neurofibromatosis type 1. Science *286*, 2176–2179.

Wang, Y., Kim, E., Wang, X., Novitch, B.G., Yoshikawa, K., Chang, L.S., and Zhu, Y. (2012). ERK inhibition rescues defects in fate specification of Nf1-deficient neural progenitors and brain abnormalities. Cell *150*, 816–830.

Ward, B.A., and Gutmann, D.H. (2005). Neurofibromatosis 1: from lab bench to clinic. Pediatr. Neurol. *32*, 221–228.

Williams, J.P., Wu, J., Johansson, G., Rizvi, T.A., Miller, S.C., Geiger, H., Malik, P., Li, W., Mukouyama, Y.S., Cancelas, J.A., and Ratner, N. (2008). Nf1 mutation expands an EGFR-dependent peripheral nerve progenitor that confers neurofibroma tumorigenic potential. Cell Stem Cell *3*, 658–669.

Woodhoo, A., and Sommer, L. (2008). Development of the Schwann cell lineage: from the neural crest to the myelinated nerve. Glia *56*, 1481–1490.

Wu, J., Williams, J.P., Rizvi, T.A., Kordich, J.J., Witte, D., Meijer, D., Stemmer-Rachamimov, A.O., Cancelas, J.A., and Ratner, N. (2008). Plexiform and dermal neurofibromas and pigmentation are caused by Nf1 loss in desert hedgehog-expressing cells. Cancer Cell *13*, 105–116.

Xu, G.F., O'Connell, P., Viskochil, D., Cawthon, R., Robertson, M., Culver, M., Dunn, D., Stevens, J., Gesteland, R., White, R., et al. (1990). The neurofibromatosis type 1 gene encodes a protein related to GAP. Cell *62*, 599–608.

Yang, F.C., Ingram, D.A., Chen, S., Zhu, Y., Yuan, J., Li, X., Yang, X., Knowles, S., Horn, W., Li, Y., et al. (2008). Nf1-dependent tumors require a microenvironment containing Nf1+/– and c-kit-dependent bone marrow. Cell *135*, 437–448.

Zheng, H., Chang, L., Patel, N., Yang, J., Lowe, L., Burns, D.K., and Zhu, Y. (2008). Induction of abnormal proliferation by nonmyelinating schwann cells triggers neurofibroma formation. Cancer Cell *13*, 117–128.

Zhu, Y., Romero, M.I., Ghosh, P., Ye, Z., Charnay, P., Rushing, E.J., Marth, J.D., and Parada, L.F. (2001). Ablation of NF1 function in neurons induces abnormal development of cerebral cortex and reactive gliosis in the brain. Genes Dev. *15*, 859–876.

Zhu, Y., Ghosh, P., Charnay, P., Burns, D.K., and Parada, L.F. (2002). Neurofibromas in NF1: Schwann cell origin and role of tumor environment. Science *296*, 920–922.